MULTIPLE LOAD CASE TOPOLOGY OPTIMIZATION BASED ON BONE MECHANICAL ADAPTATION THEORY

Emil NUȚU[1]

This paper presents structural optimum topologies for a 2D reference structure subjected to single, two and three static load cases. The topologies are determined using finite element simulations and the theory of adaptive bone remodeling, with the spatial influence function. The mechanical stimulus is the local strain energy density. It is demonstrated that, the adaptive bone remodeling theory is able to generate structural optimum topologies for multiple static load cases.

Keywords: bone mechanical adaptation, finite element, strain energy density, topology optimization, multiple load case

1. Introduction

Topology optimization (TO) methods [1-3] are used in structural design in order to determine optimal material distributions within given domains, under certain objectives, such as minimum compliance. Using the finite element method (FEM), the solutions are fictitious density distributions, i.e. relative density values between 0 and 1, where 1 corresponds to the finite elements where material should be placed and 0 to the ones where material should be removed. Graphically, the solutions are presented using density distributions plots, usually black and white representations (black for the areas with material having the unit density).

As living structures, bones are able to auto-optimize in the sense the engineering problem of TO is thought, through a process generally known as adaptive bone remodeling or bone mechanical adaptation (BMA). The literature offers several mathematical theories, e.g. [4-6], developed to model the BMA which were successfully applied to mechanical analysis, design and optimization of prosthetic implants [7-9], in conjunction with FEM. The solutions are expressed in terms of density distributions, as in TO problems.

Recently, the similarity between the BMA theory and TO was investigated [10] and the applicability of BMA to the optimization of mechanical structures was discussed [11]. Also, an interpretation of the parameters in the strain energy density (SED) based equation of BMA was given [12], under the purpose of applying it to TO problems.

In the field of TO, an important issue is to determine optimum structural solutions that should satisfy multiple loading cases. Nowak [11] emphasized that

[1] Lecturer, Strength of Materials Department, University POLITEHNICA of Bucharest, email: emil.nutu@upb.ro

the BMA simulations can be used to model multiple load case TO, but did not presented an associated methodology. In this paper, a method which is applied in BMA simulations for static modeling the dynamic loading of bones is adopted for TO of inert structures. A numerical example is studied in order to test the applicability of this method.

2. Bone adaptation theory

For the objective of this paper, it is applied the SED theory of BMA with a spatial influence function (SIF) developed by Mulender et al. [4]. The parameters involved within the simulations are based on the interpretation given in [12] for application to TO. The basic equation is [4]:

$$\frac{d\rho(x,t)}{dt} = B\phi(x,t) \tag{1}$$

where $d\rho(x,t)/dt$ quantifies the variation in time of the apparent density at the location x, B is a constant which controls the speed of the adaptation process and ϕ is the mechanical stimulus which guides the bone cells to form or to resorb bone. It is assumed that in each spatial location, the stimulus is determined by several sensor cells which are found in a certain vicinity. In the original model of Mulender et al. [4], the analysis domain was discretized with equally spaced points, to play the role of sensor cells. For each spatial location, the stimulus was calculated taking into account the contribution of all the sensors within the model. In order to reduce the computational cost, Nutu [12] introduced a parameter to control the number of sensors which contribute to the mechanical signal calculation. In this paper, this parameter, named radius of influence (RIF), is also adopted. In the following, it will be denoted with R.

At the spatial location x, the mechanical stimulus is calculated as [4]:

$$\phi(x,t) = \sum_{i=1}^{N} f_i(x)\,[S_i(t) - S_o], \tag{2}$$

with N being the number of the sensors within the vicinity defined by RIF, $S_i(t)$ is the strain energy per unit of mass (SEM) determined by the sensor i and S_o is the equilibrium value of the mechanical stimulus. The SEM is evaluated based on the the SED, $U_i(t)$, and the apparent density $\rho_i(t)$, at the location of the sensor i, according to [4]:

$$S_i(t) = \frac{U_i(t)}{\rho_i(t)}. \tag{3}$$

The SIF, $f_i(x)$, quantifies the influence upon the mechanical signal of each sensor, i, found within the vicinity of x. Its expression is:

$$f_i(x) = e^{-[d_i(x)/D]}. \tag{4}$$

According to Mulender et al. [4], the parameter D in equation (4) is defined as the distance to which the mechanical signal influence reduces with 36,8%, i.e. the SIF takes the value e^{-1}. For the TO of inert structures, this parameter, together with RIF can be used to reduce the number of finite elements that contribute to the mechanical signal while keeping the same topological solution [12].

The change in density according to equation (1) determines a change in the material Young modulus via empirical correlating functions [13]. In this paper, the relative density is used based on the argumentations given in [12]. Therefore, the Young modulus is updated according to:

$$E = E_o \rho^m, \text{ with } 0 < \rho \leq 1, \tag{5}$$

where E_o is the elasticity modulus of bulk material, i.e. the one with unit relative density.

In the above description, the calculation of SED corresponds to a single load case. In order to account for a more detailed loading configuration, which better models the dynamics of bones, Carter et al. [14] proposed the use of a strain energy functional for the calculation of the mechanical signal. In this way, they assumed that the mechanical stimulus sensed by bone cells is a cumulative information which comes from all the relevant loading configurations. Following Carter et al., Petterman et al. [15] used a similar approach imposing three relevant load cases taken from a gait cycle in the simulation of BMA in a plane model of the proximal femur. Quantitatively, the mechanical signal, S, was calculated based on:

$$S(x,t) = \left[\sum_{l=1}^{NL} \frac{n_l}{\sum_{q=1}^{NL} n_q} {U_T}_l^u(x,t)\right]^{\frac{1}{u}}, \tag{6}$$

where NL is the number of loading cases, n_l and n_q designate the number of cycles corresponding to load cases l and q, $U_{T_l}(x,l)$ is the SED at the tissue level (no pores included) determined at location x during iteration counted by t, and u a weighting parameter measuring the degree of influence of the loading configuration described throughout the NL loading cases. For a single loading configuration, u was taken as unity [14]. The conversion of U_T to the apparent level was done based on a relation similar to (3).

3. Methods

The theory presented above was implemented in a code based on MATLAB 7 and ANSYS 15 capabilities, following the procedure described in paper [16]. The values of the parameters involved within the simulation are presented in the Table 1 and are based on the interpretations given in [12]. The adaptation equation is integrated using forward Euler scheme. Thus, the density update is given by:

$$\rho_{n+1} = \rho_n + hB \sum_{i=1}^{N} f_i(x) \left[S_i(n) - S_o\right], \tag{7}$$

where h is the integration step and n is the iteration index.

Table 1

The values of the BR theory parameters considered within the simulation

B [MPa^{-1}]	h	D [mm]	R [mm]	S_o [MPa]	ρ_o	E_o [MPa]	m
1	0.01	1	3	0.43	1	10000	3

In order to combine different load cases, the method described by expression (6) is adapted for the inert structure optimization under static loads. First, notice that the correlation of load case participation with some biological aspect of cell sensing has no meaning. Second, from the mechanical design perspective, the number of loading cycles corresponding to each load case is rather a fatigue issue, which is not implied herein. In this respect, the significance of weighting parameters is not correlated with the number of cycles per load case. Based on the above mentioned observations and taking u=1, the mechanical signal calculation at the location x becomes:

$$S(x,t) = \frac{\sum_{l=1}^{NL} p_l U_l(x,t)}{\rho(x,t)}, \tag{8}$$

where p_l is the weighting parameter of the l load case, which replaces the ratio $\frac{n_l}{\sum_{q=1}^{NL} n_q}$ from expression (6).

In order to account for the contribution of N sensors to the mechanical signal calculation, one can adapt the formula (8) as follows:

$$S_i(t) = \frac{\sum_{l=1}^{NL} p_l U_l(t)}{\rho(x,t)}, \tag{9}$$

where $S_i(t)$ becomes the signal determined at the location of the sensor i, as a cumulative participation of each load case. Then, the total mechanical signal at the location x is determined based on relation (2).

Note that, the definition (8) does not restrict the sum of p_l (l=1..NL) to unity. These parameters become arbitrary numbers that can be used to determine potential different topological solutions for the same load cases, but for different participation of each. This aspect is verified within the paper as follows: for two combinations of loading, each load case weighting parameter is varied between 0.1 and 0.9, keeping the sum equal to 1. Then, the sum is allowed to vary while the ratio is kept constant.

4. Numerical example

The simulation is performed on a plane structure, by considering three different load cases. The first one corresponds to a reference Mitchel type structure, as depicted in Figure 1, a. The other two load cases are defined according to Figure 1, b and c. First, each load case is applied independently. Then, combinations of two and all three are considered.

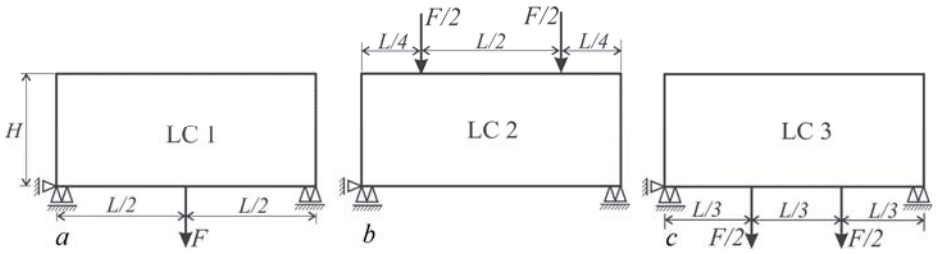

Fig. 1The test structure with the three applied load cases

The plate dimensions are H = 20 mm and L = 50 mm. Based on the Nutu rationale [12], the value of reference SEM, S_o = 0.43 MPa, corresponds to a von Mises stress of 100 MPa, produced in the material with the unit relative density. Therefore, one can expect a final stress distribution around this value, defined formally as an admissible limit, σ_a. Note, however, that this value is only a guiding reference. It is unlikely to achieve such a limit in all the finite elements describing the final topology, due to the many constraints the problem of optimization has to fulfill. More, substantial deviations from this value are expected, depending on structure configuration, load values, local stress concentrations and non-smoothness of obtained topological solution. But, as discussed in [12], the interval of von Mises stresses can be constrained to contain the admissible limit by modifying the threshold S_o. On the other hand, the solution given by the topology optimization problem is not final. During the structural design process, a stress analysis is further needed, usually followed by shape and/or size optimization.

The applied forces and the supports, in each case, are distributed on sets of nodes rather than a single node, in order to diminish the local stress concentrations. A length of 2 mm for each boundary condition distribution was imposed. The value of the force, $F = 400\ N$, is selected as in Nutu [12], because it produces von Mises stresses within the initial structures (constant density over the entire domain) under σ_a, in the areas far enough from the boundaries where conditions are imposed (forces and supports).

5. Results and discussions

In Figure 2 the final density distributions determined independently for the three load cases are presented. The black and white areas correspond to elements of density equal to 1 and 0.01, respectively. The resemblance between the first load case solution and the ones from other published results [17, 18] for the same structure is verified, validating thus the correctness of the implemented algorithm.

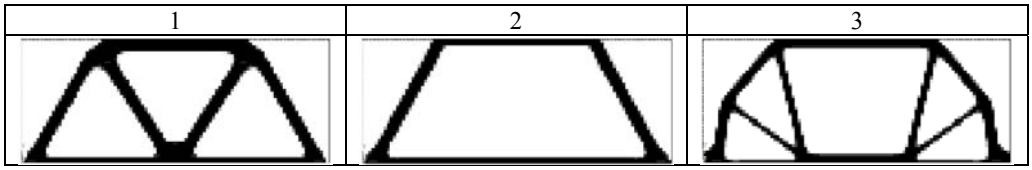

Fig. 2 Density plots determined for the three load cases independently

In order to test the capacity of the theory and the associated algorithm to produce different topologies if multiple load cases are applied, several simulations are performed based on combinations of two and all the three loading configurations. Fig. 3 shows the final density distributions obtained with such combinations.

In all plots shown in Figure 3, the contributions of each load case were equally defined, i.e. the weighting coefficients are equal. Their sum is unity. It is evident that the solutions presented are different from each of the loading cases taken independently. One can also notice, by comparison with the results from Fig. 2, that the final solution tends to adapt towards a shape that satisfies all the applied load cases.

Fig. 4 depicts density plots for different values of the weighting parameters selected such that their sum to be equal to 1. For a given load case combination, although some similarity exists, the solutions are defined by different material layouts. Thus, the combination of the weighting parameters can lead to structural solutions with different shapes.

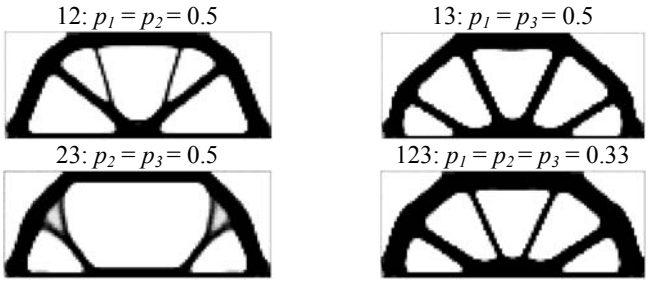

Fig. 3 Density plots determined for combinations of the three load cases with equal participation; the numbers showing the load case combination and the weighting parameter of each load case are indicated above the pictures

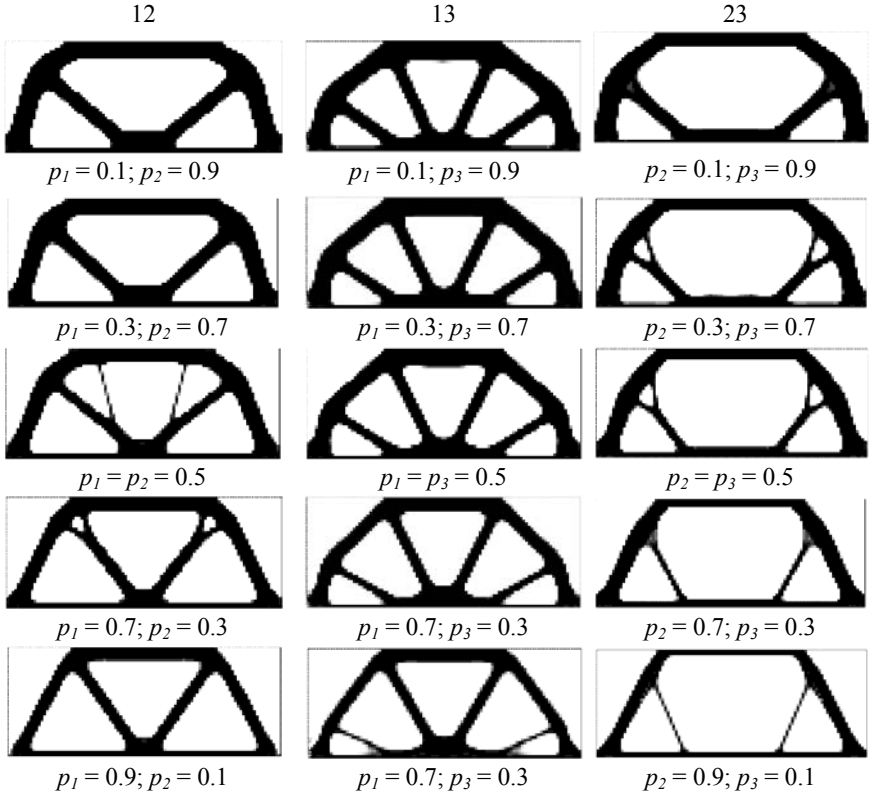

Fig. 4 Density plots determined for combinations of the three load cases with different weighting parameters; the numbers showing the load case combination are indicated above the columns and the weighting parameters are indicated below each picture

For further analysis, it is selected the ratio $p_l/p_k = 3/7$ to be kept constant, where l and k are indexes of load cases. The sum, $p_l + p_k$, is varied between 0.5

and 2. Such an approach allows to verify whether the shape of the solution is maintained under a constant participation ratio. Indeed, the results presented in Fig. 5 demonstrate this assumption. The solutions from Fig. 4 corresponding to $p_l = 0.3$ and $p_k = 0.7$ are redrawn for completeness. One can notice that, for all the variants presented, the shape is kept while the struts thickness is increased. Therefore, if the weighting parameters are varied proportionally, a size optimization can be performed. Note, however, that size optimization does not necessarily involves the modification of the whole structure dimensions. Only the dimensions of certain parts of the structure can be allowed to vary. Such an approach, however, cannot be performed by the algorithm presented herein. This is rather an issue that should be addressed by means of the next steps in the design process, which are not considered in this paper.

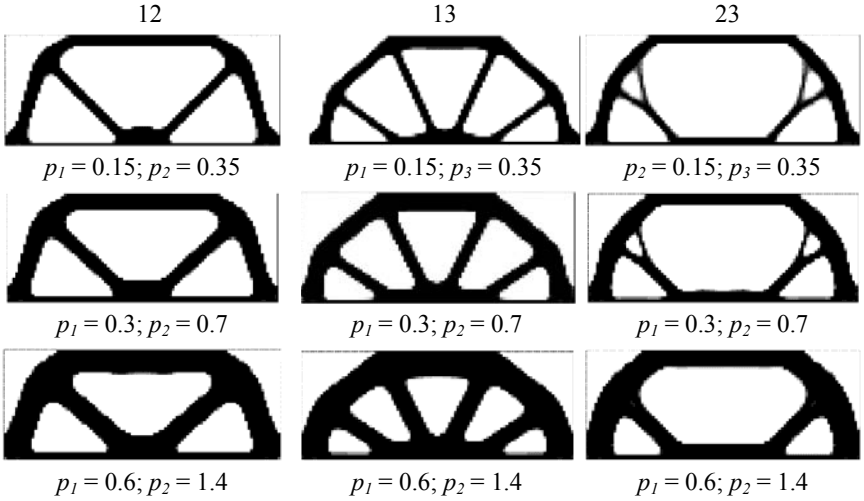

Fig. 5 Density plots determined for combinations of the three load cases with constant ratio of the weighting parameters; the numbers showing the load case combination are indicated above the columns and the weighting parameters are indicated below each picture

6. Conclusions

The results presented in this paper demonstrate that the BMA theory is able to produce optimum structural topologies for multiple load cases. Different material layouts are obtained for the same load cases combination by using weighting coefficients, which account for load case participation. Although no dynamical effect is considered, i.e. fatigue effects, the load case participation is relevant because different topological solutions can be achieved.

A global size optimization can be performed by proportionally rescaling the weighting coefficients.

In practical applications, each topological solution could serve as a start configuration for designing structures which should withstand several static load cases. By applying subsequent local size optimization, one can chose, between several variants, the one which better accomplishes a certain objective, such as minimization of structural compliance or minimization of total mass. Another practical utility of the results presented in this work could relate to the technological implications of achieving the final design. In this regard, some solutions may involve lower development costs. However, in order to be fully applicable in the industry, the theory and the associated algorithm presented in this paper should be further developed. In this respect, important directions of research include fatigue effects, stress raisers and diminishing computational time.

Acknowledgement

The work has been funded by the Sectorial Operational Programme Human Resources Development 2007-2013 of the Romanian Ministry of European Funds through the Financial Agreement POSDRU/159/1.5/S/134398.

R E F E R E N C E S

[1] *H.A. Eschenauer, N. Olhoff,* Topology optimization of continuum structures: a review, Appl Mech Rev, **vol. 54**, no. 4, Jul 2001, pp. 331 – 390.

[2] *G.I.N. Rozvany*, A critical review of established methods of structural topology optimization, Struct Multidisc Optim, **vol. 37**, issue 3, Feb 2008, pp. 217-237.

[3] *P.A. Browne*, Topology optimization of linear elastic structures, PhD Thesis, University of Bath, May 2013.

[4] *M.G. Mullender, R. Huiskes, H. Weinans,* A physiological approach to the simulation of bone remodeling as a self-organizational control process*,* J Biomech, **vol. 27**, no. 11, Nov 1994, pp. 1389-1394.

[5] *M.G. Mullender, R. Huiskes*, Proposal for the regulatory mechanism of Wolff's law, J Orthop Res, **vol. 13**, issue 4, Jul 1995, pp. 503-512.

[6] *R. Huiskes, R. Ruimerman, G.H. van Lenthe, J.D. Janssen*, Effects of mechanical forces on maintenance and adaptation of form in trabecular bone, Nature, **vol. 405***,* June 2000, pp. 704-706.

[7] *R. Huiskes, H. Weinans, H. J. Grootenboer, M. Dalstra, B. Fudala* and *T.J. Slooff*, Adaptive Bone-Remodeling Theory Applied to Prosthetic-Design Analysis, J Biomech, **vol. 20,** 1987, pp.1135-1150.

[8] *H.Y. Chou, J.J. Jagodnik, S. Müftü*, Predictions of bone remodeling around dental implant systems*,* J Biomech, **vol. 41**, no. 6, 2008, pp. 1365-1373.

[9] *H. Gong, L. Kong, R. Zhang, J. Fang, M. Zhao*, A femur-implant model for the prediction of bone remodeling behavior induced by cementless stem*,* J Bionic Eng, **vol. 10**, 2013, pp. 350-358.

[10] *I.G. Jang, I.Y. Kim, B. M. Kwak*, Analogy of strain energy density based bone remodeling algorithm and structural topology optimization, J Biomech Eng, **vol. 131**, Jan 2009, 011012.

[11] *M. Nowak*, On some properties of bone functional adaptation phenomenon useful in mechanical design, Acta Bioeng Biomech, **vol.12**, no. 2, 2010, pp. 49-54.

[12] *E. Nuțu*, Interpretation of parameters in strain energy density bone adaptation equation when applied to topology optimization of inert structures, paper submitted to Mechanika, Lithuania, in April 2015.
[13] *B. Helgason, E. Perilli, E. Schileo, F. Taddei, S. Brynjólfsson, M. Viceconti*, Mathematical relationships between bone density and mechanical properties: A literature review, Clin Biomech, **vol. 23**, Feb 2008, pp. 135-146.
[14] *D.R. Carter, D.P. Fyhrie, R.T. Whalen,* Trabecular bone density and loading hystory: regulation of connective tissue biology by mechanical energy, J Biomech, **vol. 20**, no. 8, 1987, pp. 785-794.
[15] *H.E. Pettermann, T.J. Reiter, F.G. Rammerstorfer,* Computational simulation of internal bone remodeling, Arch Comput Method E, **vol. 4**, no. 4, 1997, pp. 295-323.
[16] *E. Nuțu, H. Gheorghiu*, Influence of the numerical method on the predicted bone density distribution in element based simulations, U.P.B. Sci. Bull., Series D. 75 (2013) 73-84.
[17] *O. Sigmund*, A 99 line topology optimization code written in Matlab, Struct Multidisc Optim, Vol. 21, pp. 120-127, Springer-Verlag, 2001.
[18] *A. Tovar*, Bone remodeling as a hybrid cellular automaton optimization process, Phd Thesis, University of Notre Dame, 2004.